

Anomalous modes and matter-wave vortices in the presence of collisional inhomogeneities and finite temperature

S. Middelkamp

*Theoretische Chemie, Physikalisch-Chemisches Institut,
Im Neuenheimer Feld 229, Universität Heidelberg, 69120 Heidelberg, Germany*

P.G. Kevrekidis

Department of Mathematics and Statistics, University of Massachusetts, Amherst MA 01003-4515, USA

D.J. Frantzeskakis

Department of Physics, University of Athens, Panepistimiopolis, Zografos, Athens 157 84, Greece

R. Carretero-González

Nonlinear Dynamical Systems Group, Department of Mathematics and Statistics,
and Computational Science Research Center, San Diego State University, San Diego CA, 92182-7720, USA*

P. Schmelcher

*Theoretische Chemie, Physikalisch-Chemisches Institut, Im Neuenheimer Feld 229,
Universität Heidelberg, 69120 Heidelberg, Germany and
Physikalisches Institut, Universität Heidelberg, Philosophenweg 12, 69120 Heidelberg, Germany*

In this work, the spectral properties of a singly-charged vortex in a Bose-Einstein condensate confined in a highly anisotropic (disk-shaped) harmonic trap are investigated. Special emphasis is given on the analysis of the so-called anomalous (negative energy) mode of the Bogoliubov spectrum. We use analytical and numerical techniques to illustrate the connection of the anomalous mode to the precession dynamics of the vortex in the trap. Effects due to inhomogeneous interatomic interactions and finite temperature are explored. We find that both of these effects may give rise to oscillatory instabilities of the vortex, which are suitably diagnosed through the perturbation-induced evolution of the anomalous mode, and being monitored by direct numerical simulations.

I. INTRODUCTION

Matter-wave vortices represent fundamental nonlinear macroscopic excitations of Bose-Einstein condensates (BECs); see e.g. the relevant reviews [1, 2, 3, 4, 5, 6]. These structures are characterized by their (nonzero) topological charge S , the phase dislocation and jump by $2\pi S$ induced by the vorticity and the concomitant vanishing of the BEC density at the vortex core. Experimental observation of matter-wave vortices was first reported in Ref. [7], using a phase-imprinting method between two hyperfine spin states of a ^{87}Rb BEC [8]. Other techniques for the generation of vortices have also been studied theoretically and implemented in experiments. In particular, stirring the BEC [9] above a certain critical angular speed [10, 11, 12] is an extremely efficient method for producing a few vortices [12] or vortex lattices [13]. Other techniques include the supercritical dragging of an obstacle through the BEC [14, 15, 16], as well as the nonlinear interference of condensate fragments [17, 18, 19, 20]. In the above studies, vortices were singly-charged (i.e., with a topological charge $S = 1$); higher-charged vortices (with $S > 1$) may also be created experimentally

[21] and could, in principle, be stable under appropriate conditions [22, 23]. Nevertheless, such higher-charged vortices are typically far less robust than the fundamental $S = 1$ vortex that is of interest here.

In this work we systematically study singly-charged vortices in a two-dimensional (2D) —so-called disk-shaped— BEC from a spectral (i.e., Bogoliubov-de Gennes) point of view. In particular, first we focus on the so-called anomalous mode of the Bogoliubov theory, characterized by negative energy [24] or negative Krein-sign [25], and elucidate its connection with the precessional motion of the vortex, if displaced from its equilibrium position (i.e., the trap center). Next, we will study how this mode is affected by the presence of different kinds of perturbations. The perturbations we consider here arise from inhomogeneous interatomic interactions, so-called collisional inhomogeneities, and finite-temperature induced dissipation.

Interatomic interactions, characterized by the s -wave scattering length, become spatially (or temporally) varying by employing either magnetic [26, 27] or optical Feshbach resonances [28, 29, 30] in a very broad range. This remarkable flexibility on the manipulation of the effective mean-field nonlinearity of BECs, has inspired a significant number of experimental and theoretical studies. Herein, we will focus on the more recently proposed “collisionally inhomogeneous” BECs, character-

*URL: <http://nlds.sdsu.edu>

ized by a spatially-dependent scattering length. In such settings, many interesting phenomena have been predicted, including adiabatic compression of matter-waves [31, 32], Bloch oscillations of solitons [31], soliton emission and atom lasers [33], enhancement of transmissivity of matter-waves through barriers [34, 35], dynamical trapping of solitons [34], stable condensates exhibiting both attractive and repulsive interatomic interactions [36] and the delocalization transition of matter waves [37]. Here we will examine how harmonic spatial variations of the scattering length (inducing a sort of a non-linear optical lattice in the system) affect the stability and ensuing dynamics of the vortex. Interestingly, we find that the anomalous mode of the vortex is differently affected by sinusoidally and sinusoidally varying nonlinearities (this turns out to be the most critical element of influence within this setting). In the former case the vortex is stable, while in the latter the vortex is subject to an oscillatory instability, emerging by the collision of the anomalous mode with another eigenmode of the system.

We also consider in our study the dissipation due to the interaction with the thermal cloud. Here we will adopt a simple phenomenological model relying on the inclusion of a phenomenological damping in the mean-field model, first introduced by Pitaevskii [38] and subsequently used in various works to describe, e.g., decoherence [39] and growth [40] of BECs, damping of collective excitations of BECs [41], vortex lattice growth [42, 43], vortex dynamics [44] (see also [18, 19]), and decay of dark solitons [45]. Importantly, inclusion of such a phenomenological damping in the Gross-Pitaevskii equation (GPE) can be justified from a microscopic perspective (see, e.g., the recent review [46]). Herein, we will show how such a finite-temperature induced dissipation affects the statics and dynamics of the vortex, by leading its anomalous mode to become immediately unstable. We will also present some interesting twists that may arise when the combined effect of thermal dissipation and spatially-dependent interatomic interactions is considered.

The paper is structured as follows. In section II, we present our analytical considerations in connection to the spectrum of a $S = 1$ vortex and its precession frequency in the trap. In section III, we examine numerically the validity of the analytical predictions, but also how these are modified in the presence of additional perturbations such as the spatially dependent nonlinearity, or the finite-temperature induced dissipative perturbation. This is done both through a systematic analysis of the Bogoliubov-de Gennes equations, as well as through the direct numerical simulations of the pertinent GPE models. Finally, in section IV, we summarize our results and discuss directions for future studies.

II. ANALYTICAL RESULTS

We first consider the simplest case in our study, namely a matter-wave vortex in a 2D BEC confined in a har-

monic trap. It is well-known that in this setting the S -charged vortex will have precisely S anomalous modes [24]; these modes, characterized by a negative energy, are also known as modes of negative Krein signature in the mathematical literature [25]. In Ref. [24] (see also the review [4]), it was argued that the single negative energy mode with $S = 1$ (which is of interest here) is responsible for the precessional motion of the vortex in the trap (in addition to being relevant for other processes such as vortex nucleation).

One of the key purposes in our study is to consider the precession in the setting described above. The three-dimensional (3D) analogue of this setting has been considered and studied analytically by means of the matched asymptotics technique in Ref. [47], while the 2D case has been studied by means of a variational approach in Ref. [48] (see more details below). Here, employing the matched asymptotics method, we derive an expression for the precession frequency in the 2D case, and provide a detailed comparison of this result with numerics pertaining to the study of the anomalous mode.

The model under consideration is the $(2 + 1)$ -dimensional GPE, which can be expressed in the following dimensionless form [6],

$$i\partial_t u = -\frac{1}{2}\Delta u + V(r)u + g|u|^2 u - \mu u. \quad (1)$$

Here, $u(x, y, t)$ is the macroscopic wave function of the disk-shaped BEC, Δ is the 2D Laplacian, $r \equiv \sqrt{x^2 + y^2}$ is the radial variable, $V(r) = \frac{1}{2}\Omega^2 r^2$ is the harmonic trapping potential, $\Omega = \omega_r/\omega_z$ is the ratio of in-plane and transverse trapping frequencies, g is the normalized strength of the interatomic interactions (which we set to $g = 1$ for the analytical considerations of this section), and μ is the chemical potential. In order to study the effect of the potential on the vortex, we will follow the lines of Ref. [49] (see also Ref. [50] for similar work in the context of optics) and use a matched asymptotics approach between an inner and an outer perturbative solution leading to the following equations of motion (for a more detailed derivation see the appendix) for the vortex center (x_v, y_v) :

$$\dot{x}_v = \frac{\Omega^2}{2\mu} \log\left(A\frac{\mu}{\Omega}\right) y_v, \quad (2)$$

$$\dot{y}_v = -\frac{\Omega^2}{2\mu} \log\left(A\frac{\mu}{\Omega}\right) x_v, \quad (3)$$

where A is an appropriate numerical factor (detailed comparison with numerics yields very good agreement in the Thomas-Fermi regime e.g. for $A \approx 8.88 \approx 2\sqrt{2}\pi$, see below). These results suggest a precession of the vortex in the harmonic trap with a frequency

$$\omega_{\text{an}} = \frac{\Omega^2}{2\mu} \log\left(A\frac{\mu}{\Omega}\right), \quad (4)$$

which, as suggested by the subscript (“an” stands for anomalous), should coincide with the eigenfrequency of

the anomalous mode of the Bogoliubov spectrum. The anomalous mode eigenfrequency can readily be derived by a standard Bogoliubov-de Gennes (BdG) analysis: this includes the derivation of the BdG equation, stemming from a linearization of the GPE (1) around the vortex solution by using the ansatz

$$u = u_0(r)e^{i\theta} + \left[a(x, y)e^{i\omega t} + b^*(x, y)e^{-i\omega^* t} \right], \quad (5)$$

and the solution of the ensuing BdG eigenproblem for the eigenfunctions $\{a(x, y), b(x, y)\}$ and eigenfrequencies ω .

Note that due to the Hamiltonian nature of the system, if ω is an eigenfrequency of the Bogoliubov spectrum, so are $-\omega$, ω^* and $-\omega^*$. Notice that a linearly stable configuration is tantamount to $\text{Im}(\omega) = 0$, i.e., all eigenfrequencies being real. One of the eigenvalues of each double pair possesses a topological property of, so-called, *negative energy* (in the physical literature) [51] or *negative Krein signature* (in the mathematical literature) [52]; practically, this means that it becomes structurally unstable, i.e., it becomes complex, upon collision with other eigenvalues. The eigenvalues with negative Krein signature are actually associated with the anomalous modes [1] appearing in the BdG spectrum.

In order to compare our results to the ones obtained in earlier works, we should mention that a similar setup was investigated in Ref. [48] (by means of a variational approximation) and the frequency of the anomalous mode was derived with a similar functional form. However, in Ref. [48], the case of a BEC unbounded in the axial direction ($\omega_z = 0$) was considered and, as a result, the constant was found to take a different value, $A = 2$. It is also worth noting that the connection between quantum fluctuations and anomalous modes of matter-wave vortices under Magnus forces was considered in Ref. [53]

It is important, at this stage, to make a few comments regarding the nature of the Bogoliubov spectrum resulting from the linearization around the vortex. The system at hand, namely the disk-shaped condensate carrying the vortex, is *not* in the ground state (a similar situation occurs in the 1D analogue of the system, namely a quasi-1D BEC carrying a dark soliton). The existence of the anomalous mode, characterized by negative energy, indicates that the vortex (and the dark soliton in the 1D case) is thermodynamically unstable and, in the presence of dissipation, the system is driven towards a lower energy configuration, namely the ground state. Also, the eigenfrequency of the anomalous mode of the vortex (similarly to the case of the dark soliton [54]) bifurcates from its value $\omega = \Omega$ (the linear oscillation with the trap frequency) in the linear limit —where the vortex is represented by the linear superposition $|1, 0\rangle + i|0, 1\rangle$, where $|m, n\rangle$ denotes the m -th linear eigenstate of the quantum harmonic oscillator along the x -direction and n -th one along the y -direction (see discussion in section III A and Fig. 1). Generally, the anomalous mode (in both 1D and 2D cases) is the *lowest* excitation frequency of the system

and the only one below the trap frequency (associated with the Kohn mode corresponding to the dipole mode of the condensate [55]). However, in the case of the vortex (and contrary to what is the case for the dark soliton), there is one more frequency (which grows monotonically away from the origin near the linear limit), which may be smaller than ω_{an} (at least for small chemical potentials). This frequency was described through a small parameter expansion in section V.B of Ref. [56]. The relevant eigenfrequency is given (in our units) by the following expression,

$$\omega \approx \mu - 2\Omega, \quad (6)$$

which becomes increasingly more accurate as $\mu \rightarrow 2\Omega$. This is in contrast to the case for the expression of the precession frequency, which should be increasingly more accurate in the Thomas-Fermi (TF) limit, corresponding to large μ .

We now turn to numerical investigations in order to examine the validity of our results in the case of the parabolic trap for constant nonlinearity strength, as well as to generalize them to settings which are less straightforward to consider by analytical means. The results will be partitioned in two subsections: firstly, we will provide bifurcation results from the BdG analysis, and subsequently, we will also test the BdG predictions against full numerical integration of Eq. (1).

III. NUMERICAL RESULTS

A. Bogoliubov-de Gennes Analysis

We start with the case of a harmonically confined BEC with homogeneous interatomic interactions (i.e., $g = 1$). In Fig. 1 we show the eigenfrequency ω of the Bogoliubov spectrum as a function of the chemical potential μ . We observe that in accordance to the analytical predictions, the lowest modes are (i) the one monotonically increasing away from zero and (ii) the anomalous mode —connected to the vortex precession (see previous section). For the monotonically increasing mode, we notice that the non-radial nature of the solutions at hand (due to their phase profile) leads to the absence of additional symmetries of the eigenvalue problem away from the linear limit. The only symmetry generally present is that of the phase or gauge invariance, associated with the conservation of the number of particles. This sustains a pair of linearization eigenfrequencies at $\omega = 0$, but as discussed in Ref. [56], at the linear limit the dimension of the corresponding kernel is 4, hence an eigenfrequency pair should depart from the origin (at least for small μ) according to Eq. (6). As observed in Fig. 1, this prediction is in good agreement with the numerical results, (naturally, deviations are observed for larger chemical potentials). On the other hand, as concerns the precession frequency, we notice its monotonically decreasing dependence on μ for given Ω (the latter, was set to $\Omega = 0.2$ in Fig. 1), its bifurcation

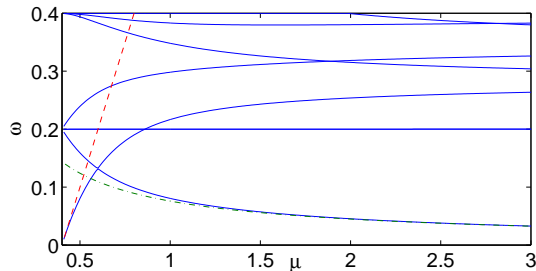


FIG. 1: (Color online) The eigenfrequency ω of the Bogoliubov spectrum as a function of the chemical potential μ (for a trap strength $\Omega = 0.2$). Theoretical predictions are given by $\omega = (\mu - 2\Omega)$ [(red) dashed line] for the mode monotonically increasing from zero and $\omega = (\Omega^2/(2\mu)) \log(A\mu/\Omega)$ [(green) dash-dotted line]; the constant A was chosen to be $2\sqrt{2}\pi \approx 8.886$.

from the Kohn mode eigenfrequency limit and its excellent agreement with the theoretical prediction in the TF limit (for all $\mu > 1$). We note in passing that in this two-dimensional case, a pair of Kohn modes can be seen to be preserved at $\omega = \Omega = 0.2$, being associated with the dipole oscillations of the condensate along the two spatial directions, while the fourth mode at 0.2 in the linear limit results in a monotonically growing eigenfrequency, as μ is increased.

We have also tested the validity of the analytical predictions concerning the two lowest eigenfrequencies for different values of Ω and as a function of μ (see Fig. 2). Once again, a very good agreement of the two asymptotic theoretical descriptions in their respective limits is found.

We now consider an interesting modification to this picture, arising from a consideration of inhomogeneous interatomic interactions, described by a spatially-dependent scattering length $a(x, y)$ (see, e.g., the recent special volume [57]). Here, we will consider the effect of a periodic variation of the nonlinearity strength, $g \equiv g(x, y)$ (i.e., a sort of a nonlinear optical lattice) on the spectrum of a vortex. We will also draw parallels with similar spectral implications in the setting of a linear periodic potential analyzed in Ref. [58].

In Fig. 3, we study the case of a *cosinusoidal* variation of the nonlinearity strength, namely, $g(x, y) = 1 + s(\cos^2(\pi x/4) + \cos^2(\pi y/4))$, monitoring the vortex spectrum as a function of the chemical potential, where s is the strength of the oscillation. In the same figure, the typical form of the density and phase of the wave function (the former showcasing spatial variation dictated by the corresponding variation of the scattering length, and the latter demonstrating the vortex structure of the configuration), as well as the Bogoliubov excitation spectrum, are also illustrated. We notice that while most of the relevant eigenfrequencies are only very weakly affected by the spatially-dependent nonlinearity, the one which is most *dramatically* affected is that of the anomalous

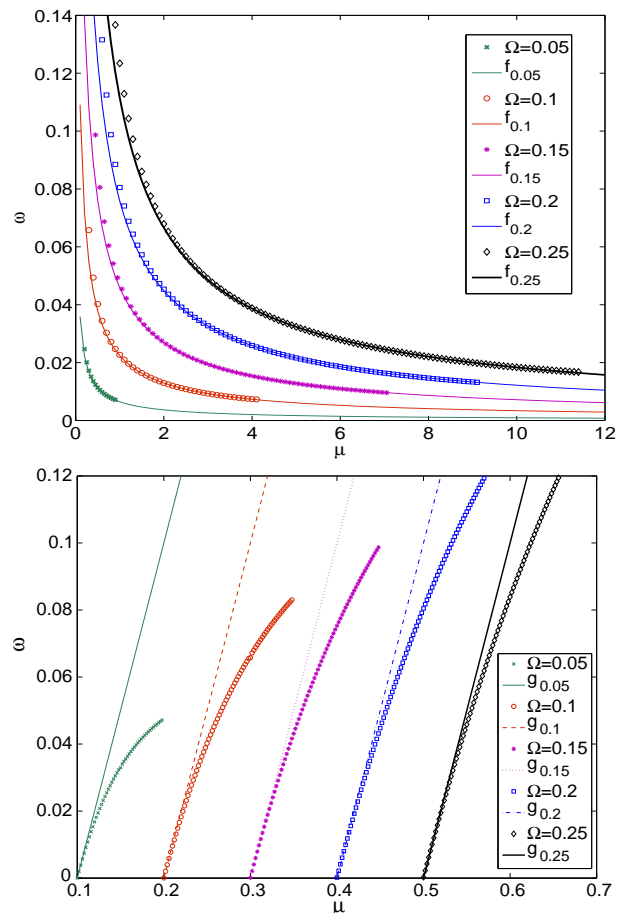


FIG. 2: (Color online) Top: dependence of the anomalous mode eigenfrequency on the chemical potential for different trap frequencies Ω . The data points are interpolated by the functions $f_\Omega(\mu) = (\Omega^2/(2\mu)) \log(2\sqrt{2}\pi\mu/\Omega)$. Bottom: similar to top panel, but for the mode bifurcating from zero, as compared to the theoretical prediction $g_\Omega(\mu) = \mu - 2\Omega$.

mode. The comparison of the $s = 0$ case of Fig. 1 (blue solid lines) with the red dashed line of $s = 0.1$ and the green dash-dotted of $s = 0.3$ illustrates that the latter two not only approach zero, but rather cross it at a finite value of μ . For $s = 0.1$, the anomalous mode hits the origin of the spectral plane at $\mu = 2.61$, while for $s = 0.3$ at $\mu = 1.56$. However, it is perhaps even more remarkable that this collision does not produce an instability through an imaginary eigenfrequency (real eigenvalue) pair, but rather maintains the stability of the configuration (the eigenfrequencies appear to go through each other). Generally, it can be seen that the trend of increasing the oscillation strength in the sinusoidal case leads to a more rapid decrease of the anomalous mode eigenfrequency with μ and an “earlier” collision (i.e., occurring for smaller μ) with the spectral plane origin.

It is now interesting to turn to the case of the *sinusoidal* modulation of the nonlinearity strength, namely $g(x, y) = 1 + s(\sin^2(\pi x/4) + \sin^2(\pi y/4))$. In this case, as observed in Fig. 4, the fundamental difference is that the

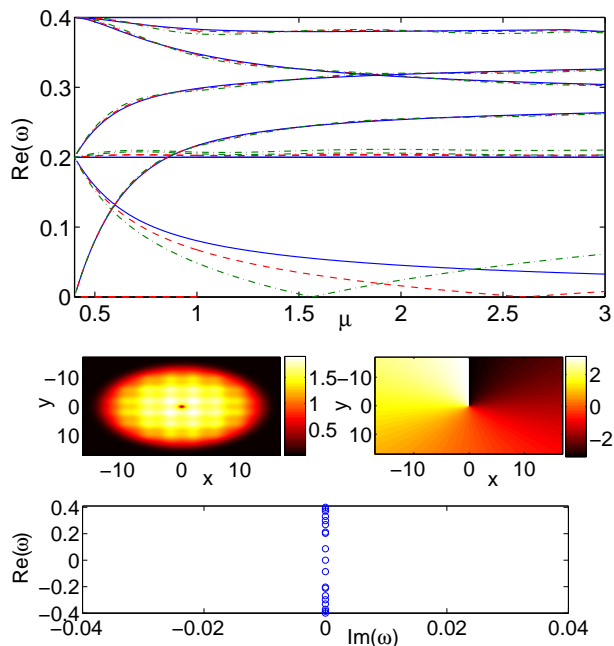


FIG. 3: (Color online) The case of a cosinusoidal variation of the nonlinearity strength. The top panel is similar to Fig. 1, the middle panels show contour plots of the density (left) and phase (right) of the wave function, while the bottom panel shows the respective Bogoliubov excitation spectrum (real vs. imaginary part of the eigenfrequency ω , where instability would correspond to the existence of eigenfrequencies with $\text{Im}(\omega) \neq 0$). The chemical potential is $\mu = 4$ (approaching the Thomas-Fermi limit). Comparison of $g(x, y) = 1 + s (\cos^2(\pi x/4) + \cos^2(\pi y/4))$, with $s = 0.1$ [(red) dashed line] and $s = 0.3$ [(green) dash-dotted line], with the case of $s = 0$ [(blue) solid line].

anomalous mode is larger than that of the homogeneous interactions case ($g = 1$). More importantly perhaps, its dependence can also be non-monotonic, resulting in the increase of the corresponding eigenfrequency for a chemical potential $\mu \gtrsim 1$. Consequently, this raises the possibility of collision of the relevant eigenmode with other modes bifurcating from $\omega = \Omega$ for sufficiently large μ ($\mu \approx 2.11$ in the case of $s = 0.3$ considered in the figure). This, in turn, produces an instability due to the opposite Krein sign of the colliding modes, yielding a quartet of complex eigenfrequencies. The (positive) imaginary part of the latter, is shown in the bottom panel of Fig. 4; see also the second and third row of panels for a typical profile and spectral plane of the relevant configuration.

The above features of the anomalous mode seem structurally similar to the linear periodic potential case, where again the cosinusoidal case was found to be dynamically stable, while the sinusoidal one was unstable beyond a critical lattice strength [58]. These results also motivate an investigation of how this phenomenology may be modified in the presence of a dissipative term.

In this case, the pertinent model is the so-called dissipative GPE, which can be expressed in the following

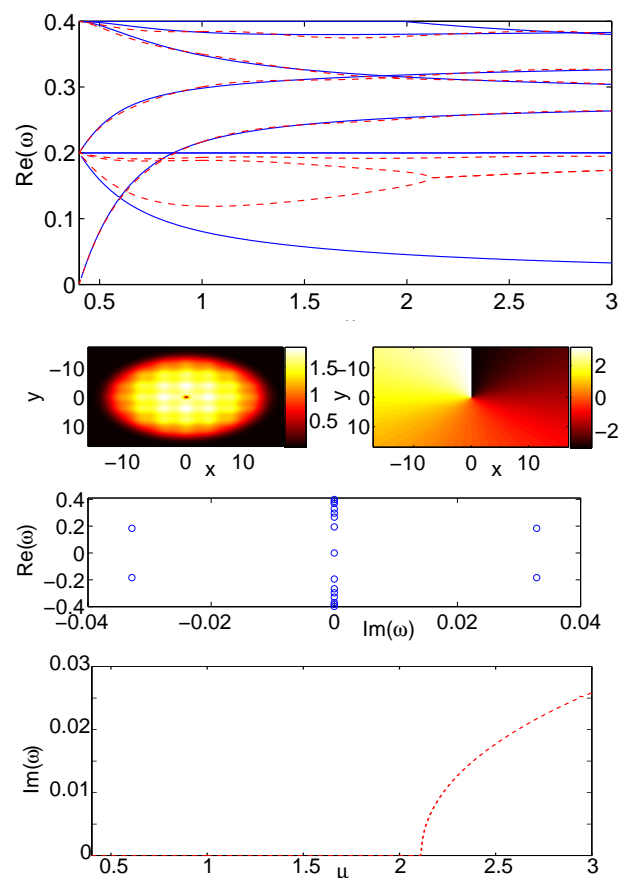


FIG. 4: (Color online) Similar to Fig. 3, but for the case of a sinusoidal variation of the nonlinearity strength. The first three rows of panels are analogous to the panels of Fig. 3. The case of $g(x, y) = 1 + s (\sin^2(\pi x/4) + \sin^2(\pi y/4))$, for $s = 0.3$ [(red) dashed line] is compared to that of $s = 0$ [(blue) solid line]. The bottom panel shows the imaginary part of the complex eigenfrequency; the oscillatory instability arises for $\mu > 2.11$.

dimensionless form:

$$(i - \gamma)u_t = -\frac{1}{2}\Delta u + V(r)u + |u|^2u - \mu u, \quad (7)$$

where the dimensionless parameter γ can be associated with the system's temperature according to [40, 43] (see also [46])

$$\gamma = G \times \frac{4ma^2k_B T}{\pi\hbar^2}, \quad (8)$$

with k_B being Boltzmann's constant and the heuristically introduced dimensionless prefactor $G \approx 3$. The chemical potential and trap strength in Eq. (7) are set to the values $\mu = 1$ and $\Omega = 0.2$ (per the above discussion, it is understood how different μ and Ω will modify the relevant phenomenology).

In Fig. 5, we show the BdG spectrum of a vortex for a case of $\gamma = 0$ (zero temperature, i.e., no dissipation)

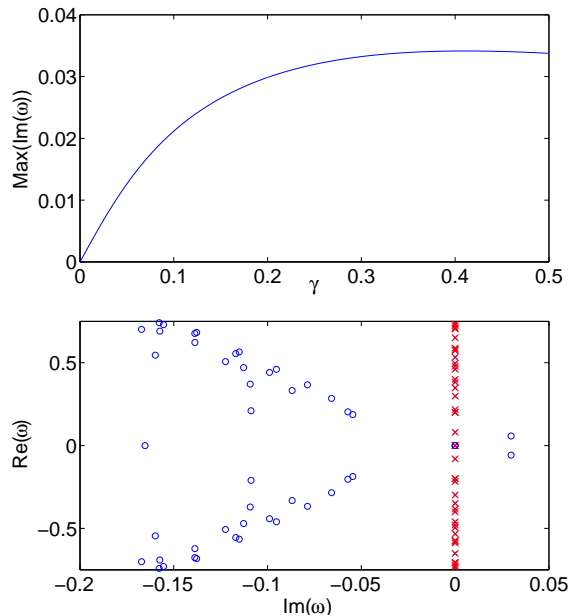


FIG. 5: (Color online) The top panel shows the immediate acquisition of a non-vanishing imaginary part of the eigenfrequency associated with the anomalous mode, as soon as the temperature-dependent dissipative prefactor γ becomes nonzero. The bottom panel highlights the special behavior of the anomalous mode by illustrating the BdG spectrum for the cases of $\gamma = 0$ (red crosses) and that of $\gamma = 0.2$ (blue circles). Notice how in the latter case the eigenfrequencies form nearly two symmetric arcs in the negative imaginary half-plane.

and for the case of $\gamma = 0.2$ (finite temperature, i.e., dissipation). It is clear that the lowest frequency mode of the condensate (which for $\mu = 1$ is the anomalous mode) is the one that, for nonzero values of γ , immediately acquires a positive imaginary eigenfrequency, contrary to what is the case for all other eigenmodes of the system. In fact, precisely this property was rigorously proved in [25] for negative Krein sign eigenmodes, namely that their bifurcation upon such dissipative perturbations happens *oppositely* to that of all other modes (of positive energy) of the system. This remarkable feature is directly consonant with the property of this excited state of the system resulting, via the effect of dissipation (and through the complex nature of the relevant eigenmode) eventually into the ground state of the system. Moreover, notice that this complex eigenmode also implies the combination of growing amplitude with the previously analyzed precessional motion, leading to the spiraling of the vortex core toward the edges of the TF cloud and its eventual disappearance, in favor of the ground state of the system (see below).

Lastly, let us investigate the effect of a periodic modulation of the nonlinearity on the stability of the system for the finite-temperature case. For a periodic cosinusoidal modulation of the nonlinearity the imaginary part of all eigenfrequencies vanishes and the system is stable for $\gamma = 0$ as discussed above. The top panel of

Fig. 6 shows the maximal imaginary part of the eigenfrequency as a function of γ for different chemical potentials μ for $g(x, y) = 1 + s(\cos^2(\pi x/4) + \cos^2(\pi y/4))$, with $s = 0.3$. For $\gamma = 0$ the imaginary part of the eigenfrequency vanishes for all cases. However, for small μ the imaginary part of the eigenfrequency becomes non-zero immediately, similar to the case of a constant nonlinearity strength. On the other hand, for large chemical potential the maximal imaginary part of the eigenfrequencies remains zero *independent* of γ . Thus, the system remains stable even in the presence of dissipation. This behavior can be understood by investigation of Fig. 4. The occurrence of a positive imaginary part of the eigenfrequencies is due to the fact that the anomalous mode is of negative Krein sign. However, for the case of a cosinusoidal modulation of the nonlinearity one observes that the value of the frequency of the anomalous mode decreases with increasing μ and, finally, even crosses the origin. At that critical point, the frequency curve shows a crossover with its opposite-value companion (of the same pair). However the latter mode has a positive Krein sign and therefore (since all negative signatures arise for negative frequencies, and positive signatures for positive frequencies), the imaginary parts of the eigenfrequencies become negative in the case of nonzero γ . The bottom panel in Fig. 6 provides an overview of the eigenfrequencies for $\gamma = 0.2$ and $\mu = 1.6$. All eigenfrequencies were shifted further into the negative imaginary half-plane in comparison to the corresponding panel in Fig. 5. Importantly, the eigenfrequencies corresponding to the (formerly) anomalous mode got shifted into the negative imaginary half-plane as is shown in the inset.

B. Direct Numerical Simulations

In this section we show results obtained by direct numerical integration of Eq. (1) starting with different initial states containing a single vortex. In order to determine the position of the vortex as a function of time we first compute the fluid velocity [15],

$$\mathbf{v}_s = -\frac{i}{2} \frac{u^* \nabla u - u \nabla u^*}{|u|^2}. \quad (9)$$

The fluid vorticity is then defined as $\omega_{\text{vor}} = \nabla \times \mathbf{v}_s$. Due to our setup, the direction of the fluid vorticity is always the z -direction and, therefore, we can treat this quantity as a scalar. Furthermore, we investigate single vortex states leading to a single maximum of the fluid vorticity at the position of the vortex. This allows us to determine the position of the vortex by determining the center of mass of the vorticity ω_{vor} .

Figure 7 shows the evolution of a single vortex for $g = 1$. We displaced the vortex initially from the center of the trap to $(x_0, y_0) = (-1.5, 0)$ and propagated the state numerically using Eq. (1). The thus obtained results are compared to the solutions of Eqs. (2)–(3) $x = x_0 \cos(Ct)$ and $y = y_0 \sin(Ct)$ with $C = (\Omega^2/(2\mu)) \log(A\mu/\Omega)$ and

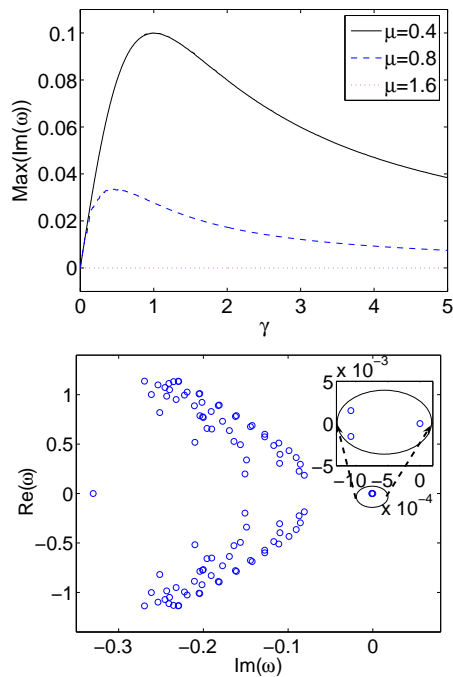


FIG. 6: (Color online) The top panel shows the immediate acquisition of a non vanishing imaginary part of the eigenfrequency associated with the anomalous mode, as soon as the temperature-dependent dissipative prefactor γ is nonzero for small chemical potentials, but no acquisition of an imaginary part for large chemical potentials. The bottom panel gives an overview of the eigenfrequencies for $\gamma = 0.2$ and $\mu = 1.6$. The maximum imaginary part is zero. The inset shows that the eigenfrequencies corresponding to the anomalous mode got shifted into the negative imaginary half-plane.

the initial position (x_0, y_0) . The theoretical predictions agree very well with our numerical findings: the vortex oscillates around the center of the trap with constant frequency and radius (see top panel). The bottom panel shows the trajectory for the case of constant nonlinearity $g = 1$ but for finite temperature (i.e., including dissipation). The results shown were obtained by direct numerical integration of Eq. (7) for $\gamma = 0.2$, with the initial condition being a slightly perturbed eigenstate of the system. Due to the instability of the system this small perturbation leads to the spiraling out of the vortex, as is physically anticipated in the presence of finite temperature [59]; we note in passing that this work contains a detailed model from microscopic first principles that illustrates a similar phenomenology upon a spatially dependent inclusion of the coupling of the condensate with the thermal cloud.

Figure 8 shows the trajectory of a vortex for the case of a periodically modulated sinusoidal nonlinearity, $g(x, y) = 1 + s(\sin^2(\pi x/4) + \sin^2(\pi y/4))$. The initial configuration is a slightly perturbed eigenstate leading to a small shift of the position of the vortex. Due to the instability of the sinusoidal $g(x, y)$ landscape, the vortex spirals outwards initially, but then spirals inwards after

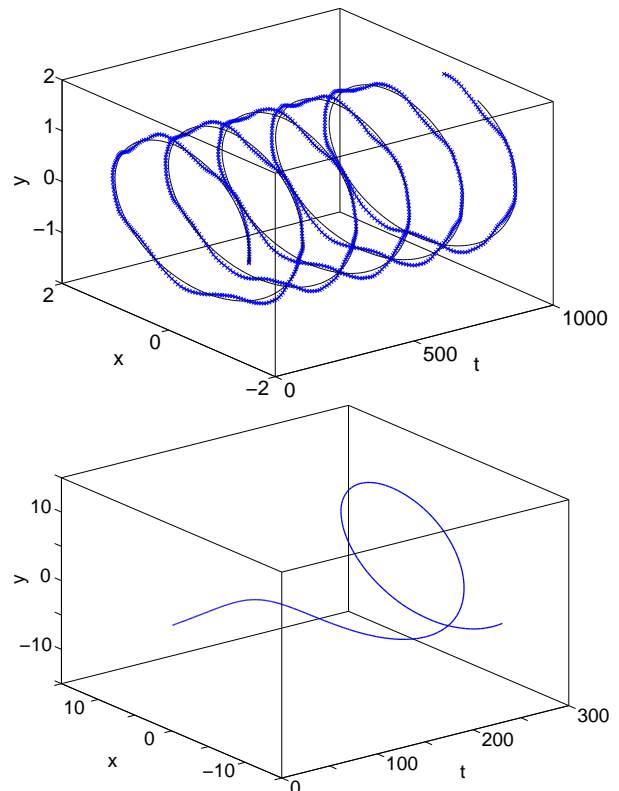


FIG. 7: (Color online) The left panel shows the trajectory of the vortex for $g = 1$ and $\mu = 3$ obtained by direct integration and the theoretical prediction obtained by solving Eqs. (2)–(3). Notice the excellent agreement between the two. The right panel shows the corresponding trajectory for the case taking into account dissipation, namely integrating Eq. (7) with $\gamma = 0.2$.

reaching a region with approximately constant nonlinearity. Subsequently the vortex follows a series of such alternating (spiraling first outwards, and then inwards) cycles in an apparently quasi-periodic orbit.

Figure 9 shows the trajectory of a vortex for the case of a periodically modulated cosinusoidal nonlinearity, $g(x, y) = 1 + s(\cos^2(\pi x/4) + \cos^2(\pi y/4))$, without dissipation (left panel) and with dissipation (right panel). In this case, small perturbations do not get amplified since the system is stable. However, a macroscopic displacement of the vortex to $(x_0, y_0) = (-1.5, 0)$ leads to the trajectories shown in the figure (see left panel). In the case without dissipation the vortex moves outwards (reaching a region outside the “square” of the first minima of the nonlinearity) and oscillates around the center on a trajectory with roughly constant nonlinearity. For the case with cosinusoidal nonlinearity *and* dissipation (see right panel), the vortex remains stable against small perturbation and does not spiral out, contrary to the case of a constant nonlinearity. Even for a macroscopical displacement the vortex moves back to the center of the trap and remains stable there. This behavior is possible because the effective potential due to the spatial variation

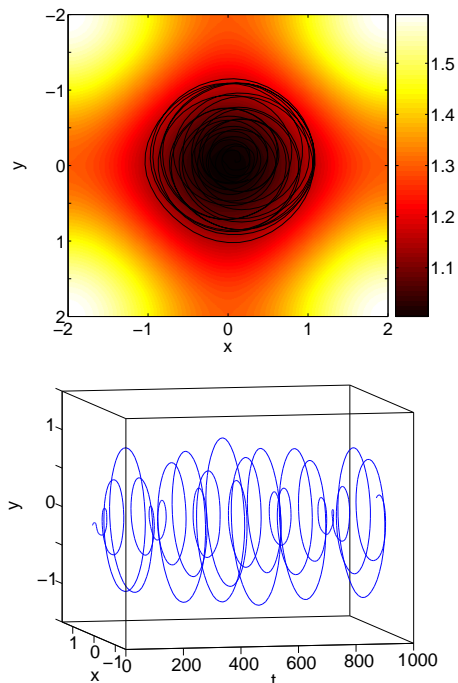


FIG. 8: (Color online) The trajectory of a vortex for $\mu = 3$ for the case $g(x, y) = 1 + s (\sin^2(\pi x/4) + \sin^2(\pi y/4))$ with $s = 0.3$. In the left panel the trajectory is plotted on top of the profile of the nonlinearity, whereas the right panel shows the trajectory as a function of time.

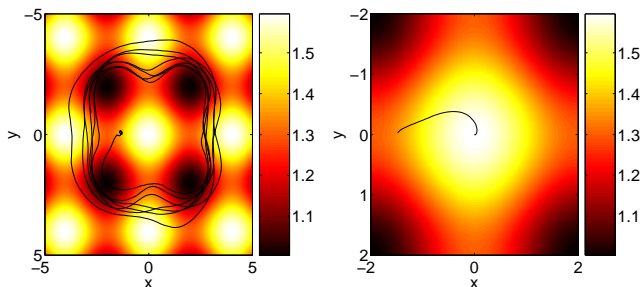


FIG. 9: (Color online) The trajectory of the vortex for $\mu = 3$ for the case $g(x, y) = 1 + s (\cos^2(\pi x/4) + \cos^2(\pi y/4))$ with $s = 0.3$ without dissipation (left) and with dissipation (right) with $\gamma = 0.2$. The trajectories are plotted on top of the profile of the nonlinearity. Notice the fast inward vortex motion in the presence of dissipation.

of the nonlinearity creates the possibility for a metastable vortex state *even in the presence of dissipation*.

In conclusion, the modulation of the nonlinearity opens up the possibility to stabilize the vortex against excitations due to finite temperature effects. This can be extremely useful for setups which require stable vortex states for a long period of time as, e.g., in the recent work of Ref. [60] which suggests the use of a superposition of two counter rotating BECs as a gyroscope.

IV. CONCLUSIONS

In summary, in the present work, we examined the role of anomalous modes in the motion of vortices in harmonically confined condensates. We have also focused on the settings of spatially dependent scattering lengths and of finite temperature (as well as the combination thereof). We found a number of interesting results, including an explicit semi-analytical expression for the precession frequency in the trap (by means of the matched asymptotics technique), which was found to be in excellent agreement with both bifurcation and direct numerical integration results, for different chemical potentials and trap frequencies within the Thomas-Fermi regime.

We subsequently examined how the spectrum (more generally —and the anomalous mode in particular) are affected by the presence of spatially-dependent (harmonic) interatomic interactions. We found that the latter may induce or avoid instabilities depending on the curvature and the strength of the nonlinearity variation. The effect of temperature was examined in a simple phenomenological setting which, however, still enabled us to observe the thermal instability of the vortex and its rapid spiraling towards the edges of the condensate cloud. Intriguingly enough, we also demonstrated that the effect of spatially dependent nonlinearities may avoid the thermal instability of the vortex by creating a local metastable effective energy minimum wherein the vortex can spiral inwards towards the center of the harmonic trap.

It would be particularly interesting to try to extend both the analytical and the numerical considerations herein towards different directions. On the one hand, it is appealing to find similar particle-like equations for the motion (and interaction) of multiple vortices within the parabolic trap. On the other hand, it would be especially relevant to consider such multi-core realizations in the presence of the thermal and spatially dependent nonlinear effects. Yet another direction could be to extend considerations presented herein to 3D settings and, in particular, to vortex rings (which are the fundamental higher-dimensional analogues of vortices considered herein). Such studies are presently in progress.

P.G.K. gratefully acknowledges support from the NSF-CAREER program (NSF-DMS-0349023), from NSF-DMS-0806762 and from the Alexander von Humboldt Foundation. R.C.G. gratefully acknowledges support from NSF-DMS-0806762. P.G.K. and S.M. acknowledge a number of useful discussions with Kody Law. The work of D.J.F. was partially supported by the Special Account for Research Grants of the University of Athens.

APPENDIX: EQUATIONS OF MOTION FOR THE VORTEX

In this Appendix we detail the effects of the potential on the position of the vortex via a matched asymptotics approach between an inner and an outer perturbative

solution. The inner solution is of the form:

$$u(r, \theta, t) = [u_0(r) + \varepsilon\chi(r) \cos(\theta)] e^{i[S\theta + \varepsilon\eta(r) \sin(\theta)]}, \quad (10)$$

where ε is a formal small parameter associated with the slow speed of precession and $u_0(r)$ is the radial vortex profile, while χ and η are functions of r , whose asymptotics have been detailed in Refs. [49, 50] (see also Ref. [47]). The outer perturbative solution can be obtained by a lowest-order equation for the phase, resulting from a rescaling of space, $r \rightarrow \varepsilon r$, and time, $t \rightarrow \varepsilon^2 t$, namely:

$$\Delta\theta + \mathbf{F} \cdot \nabla\theta = 0, \quad (11)$$

where $\mathbf{F} = \nabla \log(|u_b|^2)$ (hereafter, boldface is used to denote vectors) and $|u_b|^2$ is the (background, hence the relevant subscript) BEC density in the absence of the vortex; notice that the density can be approximated in the Thomas-Fermi (TF) limit as $|u_b|^2 = \mu - V(r)$.

Interestingly, the similarity of Eq. (11) to Eq. (20) of Ref. [50] could lead to the impression that the detailed formalism of [50] could be blindly followed giving rise to the precessional motion of Eq. (27) therein. However, this turns out to be incorrect. Particularly, in Ref. [50], it was non-generically assumed that \mathbf{F} of the outer expansion can be accurately approximated by a constant. In our case where $\mathbf{F} \approx -\Omega^2 \mathbf{r}/\mu$ (for small and intermediate distances where the matching with the inner expansion is performed), this approximation is clearly not an appropriate one. Instead, we follow the original formulation of [49], which employs the change of variables

$$\theta_x = -S \left(\phi_y - \phi \frac{\Omega^2}{\mu} y \right), \quad (12)$$

$$\theta_y = S \left(\phi_x - \phi \frac{\Omega^2}{\mu} x \right), \quad (13)$$

(we will suppress the S -dependence hereafter, focusing on singly-charged vortices). Then, the equation for ϕ reads:

$$\Delta\phi - \frac{\Omega^2}{\mu}(x\phi_x + y\phi_y) - 2\frac{\Omega^2}{\mu}\phi = 0, \quad (14)$$

which, upon using the transformation $\phi = H(r)/\sqrt{\mu - V(r)}$, yields

$$\Delta H - \frac{\Omega^2}{\mu}H = 2\pi\delta(\mathbf{r} - \mathbf{r}_0), \quad (15)$$

assuming a point vortex source at \mathbf{r}_0 . This leads to the asymptotic behavior $H = -K_0(m|\mathbf{r} - \mathbf{r}_0|)$, where K_0 is the modified Bessel function and $m = \Omega/\sqrt{\mu}$. This should be directly compared with Eq. (23) of Ref. [50], showcasing that instead of $F^r/2$ in the latter equation, here we have the constant factor m multiplying the distance from the vortex core. Once this *critical* modification is made, the rest of the calculation of Ref. [50] can be followed directly, yielding the final result (in the presence of the trap):

$$\dot{x}_v = \frac{\Omega^2}{2\mu} \log\left(A\frac{\mu}{\Omega}\right) y_v, \quad (16)$$

$$\dot{y}_v = -\frac{\Omega^2}{2\mu} \log\left(A\frac{\mu}{\Omega}\right) x_v, \quad (17)$$

where the pair (x_v, y_v) defines the location of the vortex center, A is an appropriate numerical factor (detailed comparison with numerics yields very good agreement in the TF regime e.g. for $A \approx 8.88 \approx 2\sqrt{2}\pi$, see Sec. II).

-
- [1] L. P. Pitaevskii and S. Stringari, *Bose-Einstein Condensation*, Oxford University Press (Oxford, 2003).
- [2] C. J. Pethick and H. Smith, *Bose-Einstein condensation in dilute gases*, Cambridge University Press (Cambridge, 2002).
- [3] P. G. Kevrekidis, D. J. Frantzeskakis, and R. Carretero-González, *Emergent Nonlinear Phenomena in Bose-Einstein Condensates*, Springer-Verlag (Berlin, 2008).
- [4] A.L. Fetter and A.A. Svidzinsky, J. Phys.: Cond. Matt. **13**, R135 (2001).
- [5] P. G. Kevrekidis, R. Carretero-González, D. J. Frantzeskakis, and I. G. Kevrekidis, Mod. Phys. Lett. B **18**, 1481 (2004).
- [6] R. Carretero-González, P. G. Kevrekidis, and D. J. Frantzeskakis, Nonlinearity **21**, R139 (2008).
- [7] M. R. Matthews, B. P. Anderson, P. C. Haljan, D. S. Hall, C. E. Wieman, and E. A. Cornell, Phys. Rev. Lett. **83**, 2498 (1999).
- [8] J. E. Williams and M. J. Holland, Nature **401**, 568 (1999).
- [9] K. W. Madison, F. Chevy, W. Wohlleben, and J. Dalibard, Phys. Rev. Lett. **84**, 806 (2000).
- [10] A. Recati, F. Zambelli, and S. Stringari, Phys. Rev. Lett. **86**, 377 (2001).
- [11] S. Sinha and Y. Castin, Phys. Rev. Lett. **87**, 190402 (2001).
- [12] K. W. Madison, F. Chevy, V. Bretin, and J. Dalibard, Phys. Rev. Lett. **86**, 4443 (2001).
- [13] C. Raman, J. R. Abo-Shaer, J. M. Vogels, K. Xu, and W. Ketterle, Phys. Rev. Lett. **87**, 210402 (2001).
- [14] T. Frisch, Y. Pomeau, and S. Rica, Phys. Rev. Lett. **69**, 1644 (1992).
- [15] B. Jackson, J. F. McCann, and C. S. Adams, Phys. Rev. Lett. **80**, 3903 (1998).
- [16] R. Onofrio, C. Raman, J. M. Vogels, J. R. Abo-Shaer, A. P. Chikkatur, and W. Ketterle, Phys. Rev. Lett. **85**, 2228 (2000).
- [17] D. R. Scherer, C. N. Weiler, T. W. Neely, and B. P. Anderson, Phys. Rev. Lett. **98**, 110402 (2007).
- [18] R. Carretero-González, N. Whitaker, P. G. Kevrekidis

- and D. J. Frantzeskakis, Phys. Rev. A **77**, 023605 (2008).
- [19] R. Carretero-González, B. P. Anderson, P. G. Kevrekidis, D. J. Frantzeskakis and C. N. Weiler, Phys. Rev. A **77**, 033625 (2008).
- [20] G. Ruben, D. M. Paganin, and M. J. Morgan, Phys. Rev. A **78**, 013631 (2008).
- [21] Y. Shin, M. Saba, M. Vengalattore, T. A. Pasquini, C. Sanner, A. E. Leanhardt, M. Prentiss, D. E. Pritchard, and W. Ketterle, Phys. Rev. Lett. **93**, 160406 (2004).
- [22] H. Pu, C. K. Law, J. H. Eberly, and N. P. Bigelow, Phys. Rev. A **59**, 1533 (1999). Y. Shin, M. Saba, M. Vengalattore, T. A. Pasquini, C. Sanner, A. E. Leanhardt, M. Prentiss, D. E. Pritchard, and W. Ketterle Phys. Rev. Lett. **93**, 160406 (2004).
- [23] M. Möttönen, T. Mizushima, T. Isoshima, M. M. Salomaa, and K. Machida, Phys. Rev. A **68**, 023611 (2003).
- [24] D. L. Feder, A. A. Svidzinsky, A. L. Fetter, and C. W. Clark, Phys. Rev. Lett. **86**, 564 (2001).
- [25] T. Kapitula, P. G. Kevrekidis, and B. Sandstede, Physica D **195**, 263 (2005).
- [26] T. Köhler, K. Goral, and P. S. Julienne, Rev. Mod. Phys. **78**, 1311 (2006).
- [27] S. Inouye, M. R. Andrews, J. Stenger, H.-J. Miesner, D. M. Stamper-Kurn, and W. Ketterle, Nature **392**, 151 (1998); J. Stenger, S. Inouye, M. R. Andrews, H.-J. Miesner, D. M. Stamper-Kurn, and W. Ketterle, Phys. Rev. Lett. **82**, 2422 (1999); J. L. Roberts, N. R. Claussen, J. P. Burke Jr., C. H. Greene, E. A. Cornell, and C. E. Wieman, Phys. Rev. Lett. **81**, 5109 (1998); S. L. Cornish, N. R. Claussen, J. L. Roberts, E. A. Cornell, and C. E. Wieman, Phys. Rev. Lett. **85**, 1795 (2000).
- [28] F. K. Fatemi, K. M. Jones, and P. D. Lett, Phys. Rev. Lett. **85**, 4462 (2000); M. Theis, G. Thalhammer, K. Winkler, M. Hellwig, G. Ruff, R. Grimm, and J.H. Denschlag, Phys. Rev. Lett. **93**, 123001 (2004).
- [29] D. M. Bauer, M. Lettner, C. Vo, G. Rempe, S. Dürr, Nat. Phys. **5**, 339 (2009).
- [30] D. M. Bauer, M. Lettner, C. Vo, G. Rempe, S. Dürr, Phys. Rev. A **79**, 062713 (2009)
- [31] G. Theocharis, P. Schmelcher, P. G. Kevrekidis, and D. J. Frantzeskakis, Phys. Rev. A **72**, 033614 (2005).
- [32] F. Kh. Abdullaev and M. Salerno, J. Phys. B **36**, 2851 (2003).
- [33] M. I. Rodas-Verde, H. Michinel, and V. M. Pérez-García, Phys. Rev. Lett. **95**, 153903 (2005); A. V. Carpentier, H. Michinel, M. I. Rodas-Verde, and V. M. Pérez-García, Phys. Rev. A **74**, 013619 (2006).
- [34] G. Theocharis, P. Schmelcher, P. G. Kevrekidis, and D. J. Frantzeskakis, Phys. Rev. A **74**, 053614 (2006).
- [35] J. Garnier and F. Kh. Abdullaev, Phys. Rev. A **74**, 013604 (2006).
- [36] G. Dong, B. Hu, and W. Lu, Phys. Rev. A **74**, 063601 (2006).
- [37] Yu. V. Bludov, V. A. Brazhnyi, and V. V. Konotop, Phys. Rev. A **76**, 023603 (2007).
- [38] L. P. Pitaevskii, Zh. Eksp. Teor. Fiz. **35**, 408 (1958) [Sov. Phys. JETP **35**, 282 (1959)].
- [39] R. Graham, Phys. Rev. Lett. **81**, 5262 (1998).
- [40] M. D. Lee and C. W. Gardiner, Phys. Rev. A **62**, 033606 (2000).
- [41] S. Choi, S. A. Morgan, and K. Burnett, Phys. Rev. A **57**, 4057 (1998).
- [42] M. Tsubota, K. Kasamatsu, and M. Ueda, Phys. Rev. A **65**, 023603 (2002); *ibid* **67**, 033610 (2003).
- [43] A. A. Penckwitt, R. J. Ballagh, and C. W. Gardiner, Phys. Rev. Lett. **89**, 260402 (2002).
- [44] I. Aranson and V. Steinberg, Phys. Rev. B **53**, 75 (1996); R. Sásik, L. M. A. Bettencourt, and S. Habib, Phys. Rev. B **62**, 1238 (2000); E. J. M. Madarassy and C. F. Barenghi, J. Low Temp. Phys. **152**, 122 (2008).
- [45] N. P. Proukakis, N. G. Parker, C. F. Barenghi, and C. S. Adams, Phys. Rev. Lett. **93**, 130408 (2004).
- [46] B. Jackson and N. P. Proukakis, J. Phys. B: At. Mol. Opt. Phys. **41**, 203002 (2008).
- [47] A. A. Svidzinsky and A. L. Fetter, Phys. Rev. Lett. **84**, 5919 (2000).
- [48] A. L. Fetter and J.-K. Kim, J. Low Temp. Phys. **125**, 239 (2001).
- [49] B. Y. Rubinstein and L. M. Pismen, Physica D **78**, 1 (1994).
- [50] Yu. S. Kivshar, J. Christou, V. Tikhonenko, B. Luther-Davies, and L. M. Pismen, Opt. Commun. **152**, 198 (1998).
- [51] D.V. Skryabin, Phys. Rev. A **63**, 013602 (2001); Phys. Rev. E **64**, 055601 (2001).
- [52] R. S. MacKay, in *Hamiltonian Dynamical Systems*, edited by R. S. MacKay and J. Meiss (Hilger, Bristol, 1987), p.137.
- [53] J. Dziarmaga and J. Meisner, J. Phys. B: At. Mol. Opt. Phys. **38**, 4211 (2008).
- [54] D. E. Pelinovsky and P. G. Kevrekidis, AMS Contemporary Mathematics **473**, 159 (2008).
- [55] F. Dalfovo, S. Giorgini, L. P. Pitaevskii, and S. Stringari, Rev. Mod. Phys. **71**, 463 (1999).
- [56] T. Kapitula, P. G. Kevrekidis, and D. J. Frantzeskakis, Chaos **18**, 023101 (2008).
- [57] Special Volume on *Nonlinear Phenomena in Degenerate Quantum Gases*, edited by V.M. Pérez-García, N.G. Berloff, P.G. Kevrekidis, V.V. Konotop, M. Lewenstein and B.A. Malomed, Physica D **238**, 1289 (2009).
- [58] K. J. H. Law, L. Qiao, P. G. Kevrekidis, and I. G. Kevrekidis, Phys. Rev. A **77**, 053612 (2008).
- [59] B. Jackson, N. P. Proukakis, C.F. Barenghi and E. Zaremba, Phys. Rev. A **79**, 053615 (2009).
- [60] S. Thanvanthri, K. T. Kapale, and J. P. Dowling, arXiv:0907.1138v1.